The Crop Journal 11 (2023) 744–755

Contents lists available at ScienceDirect

The Crop Journal

journal homepage: www.keaipublishing.com/en/journals/the-crop-journal/

BEAR1, a bHLH transcription factor, controls seedling growth by regulating gibberellins biosynthesis in rice

Yantong Teng [a,b,1], Maohong Cai [a,1], Qinyu Xie [a], Qinglong Liu [c], Haiwen Zhang [d], Tao Chen [a,*]

[a] Zhejiang Provincial Key Laboratory for Genetic Improvement and Quality Control of Medicinal Plants, College of Life and Environmental Science, Hangzhou Normal University, Hangzhou 311121, Zhejiang, China
[b] College of Life Sciences, Inner Mongolia University, Hohhot 010021, Inner Mongolia, China
[c] Institute of Crop and Nuclear Technology Utilization, Zhejiang Academy of Agricultural Sciences, Hangzhou 310021, Zhejiang, China
[d] Biotechnology Research Institute, Chinese Academy of Agricultural Sciences, Beijing 100081, China

ARTICLE INFO

Article history:
Received 15 November 2022
Revised 5 February 2023
Accepted 20 February 2023
Available online 21 March 2023

Keywords:
Rice
BEAR1
Seedling growth
Gibberellins
OsKS4

ABSTRACT

The genetic pathways of rice seedling growth have a major impact on seedling emergence from soil and development. In this study, we identified a new bHLH transcription factor, BEAR1, from rice RNAi mutant library. Both the *BEAR1*-RNAi and *bear1* CRISPR mutants had accelerated seedling growth. Histological section of leaves showed accelerated development of lacuna and vascular bundles in *bear1* mutant. GUS staining revealed that *BEAR1* was highly expressed in coleoptiles and leaves at seedling stage. Expression analysis of gibberellin (GA) biosynthesis and metabolic genes and content determination of active GAs indicated that the expression of GA biosynthesis genes, especially *OsKS4* and *OsCPS2*, were upregulated and the GAs content were significantly increased in *bear1*, which correlated with the seedling phenotype of *bear1* mutant. Molecular and biochemical assays revealed that BEAR1 directly binds to the promoter of *OsKS4*, thereby repressing its expression. Haplotypes analysis showed clear differentiation in *indica* and *japonica* rice varieties, and a strong correlation with seedling height. These findings provide novel insights into the regulation of seedling growth in rice.

1. Introduction

Rice is a primary food crop that feeds billions of people around the world. As labor costs increase, the cultivation pattern of rice is shifting from seedling transplanting to direct sowing, where rapid seedling growth and fast sprouting from the soil are vital for the emergence rate and yield. Seedling growth and development are the basis of rice tillering and reproduction [1]. Rice seedling possesses a coleoptile, which shields the plumule, and a mesocotyl. The length of both the mesocotyl and coleoptile is determined by a combination of genetic and environmental factors. Many genes were identified as key players in early seedling growth. OsWRKY50 mediates seedling growth via ABA-dependent pathway [2]. bZIP72 promotes rice seedling elongation by activating *ADH1* expression [3]. OsDSK2a (DOMINANT SUPPRESSOR of KAR2) mediates seedling growth by regulating GA metabolism [4]. OsRTH1 affects seedling growth by controlling ethylene-induced coleoptile elongation [5]. SnRK1A protein kinase regulates seedling growth in rice by involving in the sugar signaling cascade [6].

Phytohormones play important roles in the regulation of plant growth and development. Of these, GA plays a pivotal role in seed germination, stem elongation, tillering [7], flower development, anther maturation and grain production [8–11]. GAs have been isolated and characterized, with over 130 gibberellic acids identified, of which GA_1, GA_3, GA_4 and GA_7, are the most biologically active. GA biosynthesis begins with geranylgeranyl diphosphate (GGDP) and is divided into three steps, catalyzed in plastid, endoplasmic reticulum and cytoplasm respectively. The plastid step involves transforming GGDP to *ent*-copalyl diphosphate (*ent*-CDP) by *ent*-copalyl diphosphate synthase (CPS), and then to *ent*-kaurene by *ent*-kaurene synthase (KS) [12]. Subsequently *ent*-kaurene was converted by *ent*-kaurene oxidase (KO) in the endoplasmic reticulum to *ent*-kaurenoic acid, and then to GA_{12} by *ent*- kaurenoic acid oxidase (KAO) [13–15]. The cytoplasm step involves converting GA_{12} into different types of GAs with varying bioactivities, mainly by GA 20-oxidase (GA20ox) and GA 3-oxidase (GA3ox) [16]. GA 2-oxidase (GA2ox) is the major responsible factor for the deactivation of GAs [17,18].

* Corresponding author.
E-mail address: chentao@hznu.edu.cn (T. Chen).
[1] These authors contributed equally to this work.

https://doi.org/10.1016/j.cj.2023.02.007

Transcription factors play a crucial role in fine-tuning the levels of GA in plant cells at different stages. LEAFY COTYLEDON 2 (LEC2) and FUSCA 3 (FUS3), inhibit GA biosynthesis and regulate embryogenesis and seed development in *Arabidopsis* by suppressing the expression of *AtGA3OX2* [19]. AGAMOUS-LIKE 15, a MADS domain transcription factor, can positively regulate the GA-deactivation gene *AtGA2OX6* during embryonic development [20]. KNOX (KNOTTED-like homeobox) class transcription factors can also inhibit the expression of *GA20OX* genes [21]. Notably, bHLH transcription factors are particularly indispensable in the regulation of GA biosynthesis and signaling; PIL5, a phytochrome interacting bHLH protein, can inhibit seed germination by regulating GA responses [22].

bHLH transcription factors are involved in a wide range of hormone metabolism, and play important roles in seed germination [22,23], root development, hypocotyl elongation, vascular tissue establishment [24], stomatal differentiation [25,26], anthocyanin synthesis, photosensitive pigment signal transduction, pollen development and flowering regulation [27–30]. The bHLH genes *GLABRA3* (*GL3*) and *ENHANCER OF GLABRA3* (*EGL3*) determine the epidermal cell fate in root development [31]; PIFs, photochrome-interacting factors, play a central role in plant morphogenesis and hypocotyl growth regulation [32–35]; KIDARI, encoding a non-DNA binding bHLH protein, represses light signal transduction [36]; BIM1, a bHLH protein, controls plant embryonic patterning through brassinosteroid pathway [37]; In JA pathway, the complex of MYB/bHLH/WD40 can participate in anthocyanin biosynthesis [38].

Here we report *OsBEAR1* (bHLH transcription factor with EAR motif 1, ID: *LOC_Os11g15210*), encoding a 459 amino acids protein localized in the nucleus, regulate sprouting from soil and development of rice seedling. We confirmed the function of *OsBEAR1* by CRISPR line and RNAi knockdown line, and revealed that OsBEAR1 control plant growth and development at seedling stage by repressing of the expression level of GA biosynthesis gene *OsKS4*.

2. Materials and methods

2.1. Plant materials and growth conditions

The rice RNAi mutant library was generated by transforming artificial miRNA constructs into the *japonica* rice cultivar Nipponbare (Nip). The *bear1* mutants in the Nip background were generated using the CRISPR method [39,40], in which the target region is 5′-GGCTCTCGTCGACCGTATCA-3′. The promoter region of *BEAR1* was amplified by using primers (Table S1) followed by cloning into the gateway entry vector pENTR-D-TOPO. The pGWB533 binary vector, were used to generate constructs for GUS reporter by LR reaction. Then, the resulting plasmids were introduced into Nip via agrobacterium-mediated transformation.

Phenotypic analysis of CRISPR mutant and RNAi seedlings of *BEAR1* was conducted using the Nip as control. Hydroponic experiments in both light and dark conditions have been performed. Light hydroponic experiment was conducted with 10 h light and 14 h darkness cycle at 28 °C, while dark hydroponic experiment was performed in 24 h of darkness at 28 °C. Additionally, seedling emergence experiments were performed in the 2-cm depth soil in 24 h of darkness at 28 °C.

2.2. Domain analysis, phylogenetic analysis and cis-elements analysis

The protein structure and conserved domain of BEAR1was analyzed by SWISS-MODEL (https://swissmodel.expasy.org/) [41], Pfam (//pfam.xfam.org/) [42] and Prosite domains database (//https://www.expasy.org/prosite/) [43]. The phylogenetic tree of 211 bHLH members in *japonica* rice from the PlantTFDB database was conducted using the Maximum Likelihood method in MEGA X with 1000 bootstrap replications for statistical support of the nodes in the phylogenetic tree [44]. All positions with < 80% site coverage were removed. The 980 bp promoter sequences of P3 fragment were used for *cis*-elements analysis by PlantCARE (https://bioinformatics.psb.ugent.be/webtools/plantcare/html/).

2.3. Histological section analysis

Histological section analysis was performed on 8-day-old seedlings of Nip and bear1 in a hydroponic experiment with a photoperiod of 10 h light and 14 h of darkness at 28 °C. The leaves of the seedlings were fixed in formalin/acetic acid/alcohol solution for 24 h, dehydrated in follow series of ethanol gradients: 75% ethanol, 85% ethanol, and 95% ethanol and then transparent in xylene of different gradients before being embedded in paraffin. The paraffin block was cut into about 8 mm thick slices for staining, the 8 mm cross sections were stained with filtered 0.1% toluidine blue Sections of the same parts of both materials were stained with ferro solid green, and then photographed using a scanner [45].

2.4. GUS staining

For GUS staining, different tissues were collected from *BEAR1* promoter-GUS reporter transgenic plants, followed by immersing tissues in staining solution (50 mmol L^{-1} sodium phosphate, pH 7.0; 10 mmol L^{-1} EDTA; 0.5 mmol L^{-1} $K_3[Fe(CN)_6]$; 0.5 mmol L^{-1} $K_4[Fe(CN)_6]$; 0.1% [v/v] Triton X-100; and 1 mmol L^{-1} 5-bromo-4-chloro-3-indolyl-b-D-glucuronic acid) for 24 h at 37 °C. After the samples were dehydrated in 75% (v/v) ethanol to remove the chlorophyll, images were taken under a stereoscopic microscope.

2.5. Quantitative real-time PCR (qPCR) for expression pattern of BEAR1 gene and GA-related genes

For the temporal and spatial expression analysis of *BEAR1* at seedlings stage, the aerial parts of Nip seedlings that grow in the hydroponic and light condition were harvested at an interval of 2 days after germination for total RNA extraction. To analysis the deferent expression levels of GA biosynthesis and metabolism genes in Nip and *bear1* mutant, the 8-day-old seedlings of two materials were harvested and used to extract total RNA. Total RNA was extracted from seedlings by using the RNA Easy Fast Plant Tissue Kit with DNaseI treatment (TIANGEN). cDNAs were synthesized by HiScript Q RT SuperMix for qPCR (Vazyme). qPCR was performed on the Applied Biosystems 7500 Fast Real-Time PCR System using *OsACT1* as control [46]. Primers used in this assay are listed in Table S1.

2.6. Quantification of endogenous active GAs

The 8-day-old seedlings of Nip and *bear1* were used for the quantification of endogenous active form of GAs, including GA_1, GA_3, GA_4 and GA_7. The GA compounds were detected by Wuhan Greensword Creation Technology Company [47]. Briefly, the appropriate amount of stable isotope-labeled GAs was added to the samples homogenized with liquid nitrogen as internal reference, extracted with acetonitrile overnight in darkness at 4 °C and infused with Fe3O4@TiO2 magnetic nanoparticles for purification. After that, the extract was determined by Liquid Chromatography Tandem Mass Spectrometry (LC-MS/MS).

Analysis of phytohormones was performed on a UPLC-ESI (+/-)-MS/MS system consisting of an AB SCIEX 4500 triple quadrupole mass spectrometer with an electrospray ionization source, a Shimadzu LC-30AD HPLC system with two 30AD pumps, a SIL-30AC auto sampler, a CTO-30A thermostat column compartment, and a

DGU-20A5R degasser. Data acquisition and processing were performed using AB SCIEX Analyst 1.6 software.

2.7. Yeast one-hybrid (Y1H) and luciferase activity assays

For Y1H, the full-length coding region (1377 bp) of *BEAR1* was cloned into the pB42AD vector, and truncated fragments of the *OsKS4* promoter including KS4-P1 (787 bp), KS4-P2 (438 bp), KS4-P3 (980 bp), KS4-P4 (153 bp), KS4-P5 (282 bp), KS4-P6 (216 bp), KS4-P7 (176 bp), and KS4-P8 (247 bp) and the fragments of *OsCPS2* promoters, including CPS2-P1 (806 bp), CPS2-P2 (823 bp), and CPS2-P3 (562 bp) were cloned into the pLacZi vector, respectively [48]. The resulting constructs were co-transformed into the yeast strain EGY48 and selected on SD/-Ura/-Trp agar medium. Colonies were finally plated onto SD/-Ura/-Trp agar medium containing raffinose, galactose, and 5-bromo-4-chloro-3-indolyl-b-D-galactopyranoside for blue color development. Primers used in this assay are listed in Table S2.

The luciferase activity assay was performed following the method with modification [49]. The full-length coding region of BEAR1 was cloned into *pCAMBIA1305* and *pCAMBIA1300* to express BEAR1-GFP and BEAR1-FLAG fusion protein. The promoter fragments of *OsKS4* were ligated into the pGreenII0800-LUC vector (Biovector, USA) to generate the corresponding reporter constructs. The tobacco leaves were then co-injected with BEAR1-GFP/FLAG and *pOsKS4:LUC* followed by incubation at 25 °C for 2–3 days. The injected leaves were sprayed with 1 mmol L^{-1} luciferin (E1601, Promega) for 5 min, and luciferase activities were measured using CCD imaging system (NightShade LB 985, Berthold). To detect the luciferase activity, we used the Dual-Luciferase Reporter Assay System (Promega, USA) and normalized the firefly luciferase activity with the internal control, Renilla luciferase (LUC/REN). Primers used for this assay are listed in Table S2.

2.8. Chromatin immunoprecipitation-qPCR assay

The ChIP assay was performed as previously described [50]. In brief, to perform ChIP-qPCR assay, the full-length coding region of BEAR1 was cloned into the *pCAMBIA1300Flag* vector to produce *p35S:BEAR1-FLAG* construction. These vectors were introduced into *Agrobacterium tumefaciens* strain EHA105. The young tobacco leaves were co-transformed with *p35S:BEAR1-FLAG* and *pOsKS4:LUC* vector. The fresh samples were cross-linked in 50 mL of 1% formaldehyde for 15 min. Then the chromatin was extracted from the samples, and DNA was sheared to 100–500 bp fragments. Anti-Flag M2 Magnetic Beads (Sigma, M8823), and protein A magnetic beads (Beyotime) were used for immunoprecipitation. The final extracted DNA was used as a template for the ChIP-qPCR assay. The ratio of IP to input was used as the result of enrichment. Primers used in this assay are listed in Table S3.

2.9. Haplotypes analysis of BEAR1

To analyze the haplotypes of *BEAR1* in controlling seedling height, the full-length encoding regions of *BEAR1* (1377 bp) were used to BLAST in RFGB database (https://www.rmbreeding.cn/). The resources of 1568 *indica* and 813 *japonica* cultivars and the data of seedling height were all collected from the RFGB database.

3. Results

3.1. Rnai library screening for early seedling growth

To analyze the functional genes involved in regulating rice seedling growth, we screened RNAi library of rice transcription factors, which was generated for targeting transcription factors with Ethylene-responsive element binding factor-associated Amphiphilic Repression (EAR) motifs, defined as conserved sequence of transcription repressor. To mimic seed germination in soil, the light was absent during seeds imbibition and seedlings growth. As shown in Fig. S1A, one line named *BEAR1*-RNAi was isolated with a faster growth rate compared to Nip. The 4-day-old etiolated seedlings of *BEAR1*-RNAi were approximately 50% higher than Nip (Fig. S1C). To investigate if the light condition affects the growth rate of *BEAR1*-RNAi, the seed germination and seedling growth were checked under light. As shown in Fig. S1B, the 12-day-old *BEAR1*-RNAi seedlings were stronger than Nip and the statistical results manifested that the seedling height of *BEAR1*-RNAi seedlings was significantly higher than Nip (Fig. S1C). To confirm the *BEAR1*-RNAi line, the RNA interference efficiency of *BEAR1* was measured by qPCR. As shown in Fig. S1D, the mRNA of *BEAR1* was reduced to < 20% of Nip.

3.2. Motif and phylogenetic analysis of the bHLH family members in rice

The result of motif analysis and phylogenetic analysis revealed that BEAR1 contains a basic Helix-loop-Helix domain, which is a characteristic of the bHLH transcription factor family (Fig. S2A). Additionally, the C-terminal region of BEAR1 has an inhibitory function motif, with LxLxL structure. To further investigate the bHLH family, a Maximum Likelihood (ML) tree for bHLH family members of *japonica* rice was constructed (Fig. S2B). Results showed that the bHLH family was classified into 11 groups, with group 4 including *BEAR1*, *OsGL3b*, *OSB1*, *OSB2*, *OsRb* and *OsRb2* related to anthocyanin metabolism.

3.3. Early seedling growth function was confirmed by bear1 CRISPR mutant

To confirm the early sprouting phenotype of *BEAR1*-RNAi line, the *bear1* mutant line was generated by CRISPR/Cas9 gene editing. *bear1* has a frameshift from the N-terminal at the 50th amino acid residue and prematurely terminated at the 143th amino acid residue, which resulting in the loss of bHLH domain. The *bear1* seedlings showed a marked increase in growth and development under both light and dark conditions (Figs. 1, S3). In the maturation stage, *bear1* and Nip showed no significant difference in plant height (Fig. S4). In the hydroponic experiment under light conditions, the most pronounced phenotypic differences between CRISPR mutant *bear1* and Nip were observed in the aerial part (Fig. 1A). Statistical analysis revealed that the primary differences between the two genotypes were in seedling height, or more specifically, heart leaf height (Fig. 1B–F). Under dark conditions, the phenotypic difference between *bear1* and Nip were even more pronounced than light condition. The hydroponic experiment showed that the phenotypic differences between Nip and *bear1* (Fig. S3A–C). The emergence experiment also showed that *bear1* seedlings grew significantly faster and higher than Nip in soil (Fig. S3D, E).

3.4. Differentiation in development of lacuna and vascular bundles

Significant developmental phenotypes between Nip and *bear1* were observed in the tissue sections. In the cross-section, the most obvious difference was in the development of lacuna: the lacuna of Nip was not yet mature (Fig. 2A, C), while the corresponding lacuna of *bear1* had developed well (Fig. 2B, D). Notably, *bear1* had one more vascular bundle than Nip, demonstrating accelerated growth and development in *bear1* mutant (Fig. 2E–H). In the longitudinal section, the cell lengths of bear1 were significantly higher than Nip, and the tissue structure of *bear1* was more complex and highly

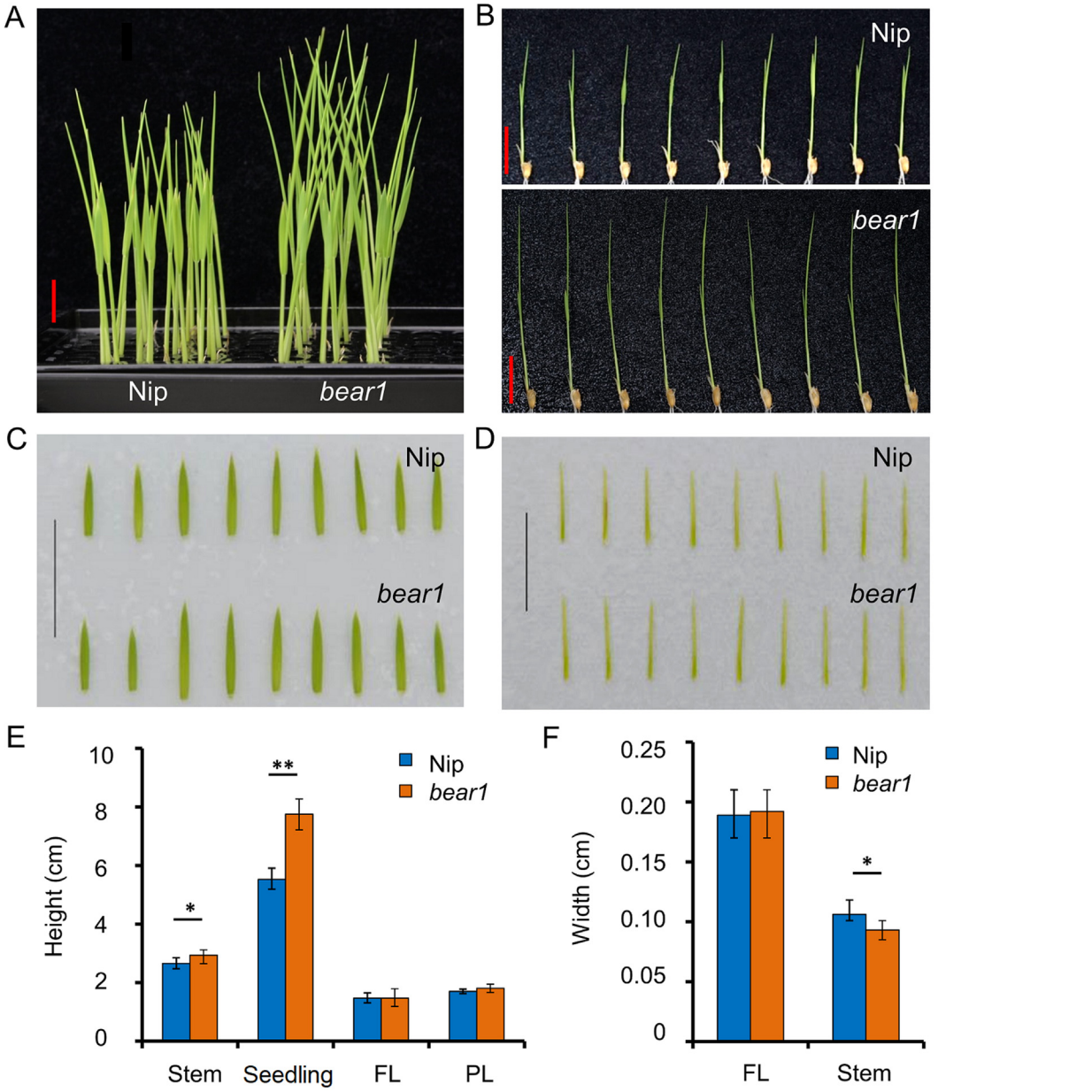

Fig. 1. Hastened growth of *bear1* seedlings under light conditions.
(A) 10-day-old seedlings of Nip and bear1 in the hydroponic experiment under the condition of 10 h light and 14 h darkness at 28 °C. (B) Seedlings of 10-day-old Nip and *bear*. (C) First leaves of 10-day-old Nip and *bear1*. (D) Leaf sheaths of 10-day-old Nip and *bear1*. (E) Height statistics of stem, seedling, FL and PL of the seedlings of Nip and *bear1*. (F) Width statistics of FL and stem of the seedlings of Nip and *bear1*. FL, first leaf; PL, primary leaf. Scale bar, 2 cm; error bars represent SD (n = 9). *, $P < 0.05$; **, $P < 0.01$ (Student's t-test).

differentiated than that of Nip, which mostly consisting of compact spongy tissues (Fig. S5).

3.5. BEAR1 participates in GA synthesis pathway

To investigate the expression pattern of BEAR1 in rice, we generated the *BEAR1* promoter-driven GUS expression construct. By agrobacterium-mediated transformation into Nip, the resulting transgenic plant was used for GUS signal detection. As shown in Fig. S6, *BEAR1* was preferentially expressed in the buds and young leaves. These results indicate that BEAR1 had a role in seedling growth of rice. To further assess the expression level of *BEAR1* during seedling stage (from day 2 to day 12 after germination), qPCR was performed and results revealed that *BEAR1* expression level increased with plant development, peaking at 8 days after germination (Fig. 3A).

To analyze the molecular mechanism of *BEAR1* in regulating seedling height, we examined the expression level of genes related to GA biosynthesis and metabolism pathways (Fig. 3B). qPCR results indicated that two GA synthesis genes, *OsCPS2* and *OsKS4*, were upregulated by 3 times compared to Nip (Fig. 3C, D). In the GA degradation pathway, four genes were slightly upregulated, and three genes were slightly downregulated (Fig. 3E).

To further confirm whether *BEAR1* affects GA biosynthesis in plant, we measured the GA contents in Nip and *bear1*. The LC-MS/MS results showed that, compared to Nip, the active GA forms including GA_1 and GA_3 in *bear1* was significantly increased, while GA_4 was slightly increased and GA_7 had no differences (Figs. 4, S7).

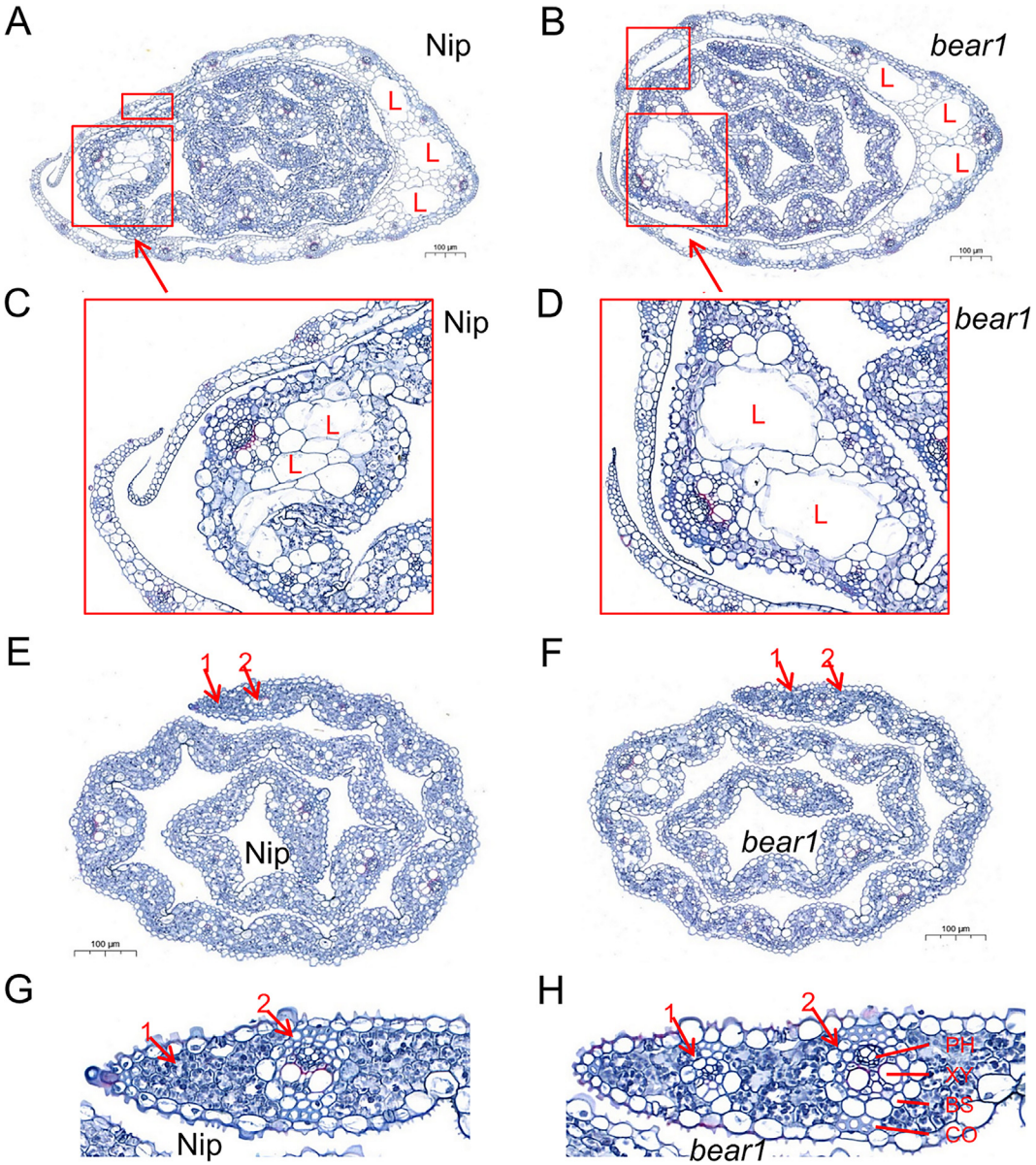

Fig. 2. Accelerated development of lacuna and vascular bundles in *bear1* mutant.
(A, B), Leaf cross section of Nip (A) and *bear1* (B). The lacuna of Nip was developing. The lacuna of *bear1* was matured. (C, D), Enlarged view of the lacuna in Nip (C) and *bear1* (D) respectively. L, lacuna. Scale bar, 100 μm. 10-day-old seedling of Nip and *bear1* were subjected to histological section. (E) Cross section of heart leaf of Nip. The red arrow 1 indicated emerging of the vascular bundle, the red arrow 2 indicated developing of the vascular bundle. (F) Cross section of heart leaf of *bear1*. The red arrow 1 indicated developing of the vascular bundle, the red arrow 2 indicated the developed vascular bundle. (G, H) Enlarged view of the lacuna in Nip and *bear1* respectively. PH, phloem; XY, xylem; BS, bundle sheath; CO, collenchyma. Scale bar, 100 μm. The area indicated by the arrow has visible differences.

To investigate whether *bear1* was sensitive to GA or GA inhibitor (Paclobutrazol, PAC), Nip and *bear1* CRISPR mutant were treated with a range of GA and PAC concentrations. For GA treatment, the seedlings height of Nip and *bear1* obviously rose with increasing GA concentrations (Fig. 5A, B). Conversely, the seedlings height of Nip and *bear1* were significantly decreased with the increase of PAC concentration (Fig. 5C, D). Interestingly, when PAC concentration was above 10 μmol L^{-1}, there was no difference in plant height between Nip and *bear1*, which indicating that the difference of plant height between Nip and *bear1* was caused by the content of GA.

3.6. BEAR1 directly binds to the promoter of OsKS4 and represses its expression

As shown in Fig. 3 and Fig. 4, *BEAR1* functions in GA signal pathway to regulate seedling height by repressing the expression of GA related genes. To further investigate whether *BEAR1* can directly bind to the promoter of *OsKS4* or *OsCPS2*, which were found to be upregulated in *bear1* mutant, Y1H and LCI assays were performed. The results of the Y1H assay revealed that *BEAR1* can indeed binds to P8 region of the *OsKS4* promoter (Fig. 6A, B), but not to the promoter of *OsCPS2* (Fig. S8). Chromatin immunoprecipitation (ChIP)-qPCR assay also showed that BEAR1 had significant enrichment in the q4 of the *OsKS4* promoter (Fig. 6C). These results revealed that BEAR1 can directly bind to the *OsKS4* promoter and repress its expression. To confirm this, we transformed different effectors into tobacco plants to test the effect of BEAR1 on *OsKS4* expression. The activity of luciferase driven by *OsKS4* promoter was significantly decreased when the BEAR1-GFP and BEAR1-FLAG protein were added, compared to the control (Fig. 6D, E). These findings suggested that BEAR1 represses the expression of *OsKS4* by directly binding to its promoter, thus regulating GA biosynthesis and seedling height.

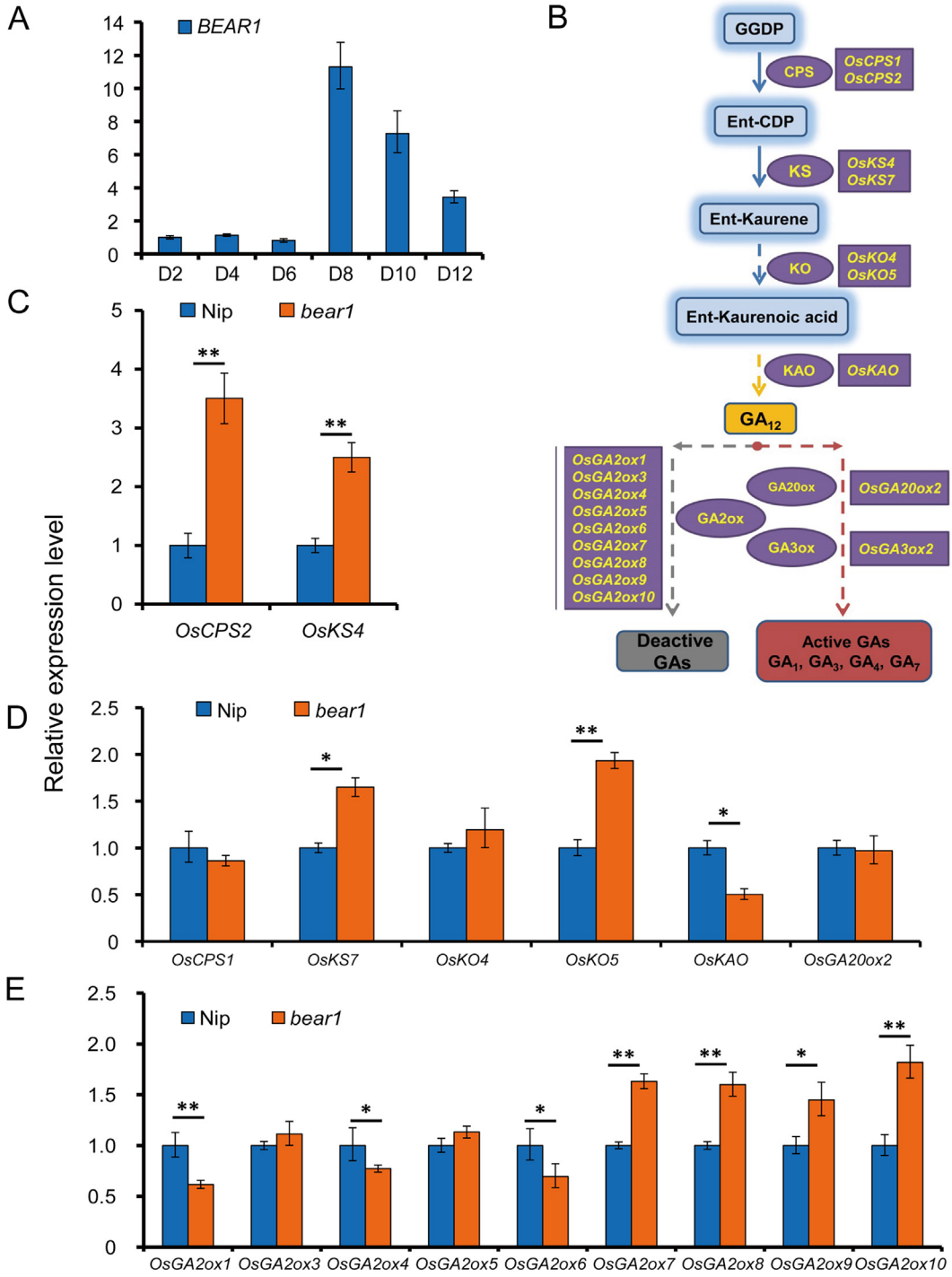

Fig. 3. GA biosynthesis and metabolism genes were differently regulated in *bear1*.
(A) Expression pattern of *BEAR1* gene. The seedlings after germination were harvested and total RNA was extracted. qPCR was performed to determine the expression levels of *BEAR1*. D2 to D12 represents the day after germination. (B) Diagram of GA biosynthesis and metabolism pathway in rice. (C, D) Expression pattern of GA biosynthesis-related genes between Nip and *bear1*. (E) Expression pattern of GA deactivation-related genes between Nip and *bear1*. Error bars represent SD (n = 3). *, $P < 0.05$; **, $P < 0.01$ (Student's t-test).

3.7. Haplotypes analysis of BEAR1 in rice cultivars

To further investigate the molecular role of *BEAR1* in controlling seedling height, we analyzed the haplotypes of 1568 *indica* and 813 *japonica* cultivars (https://www.rmbreeding.cn). The full-length encoding regions of *BEAR1* (1377 bp) were used to identify 9 SNPs, 4 of which caused changes in amino acid sequence in cultivars (Fig. 7A). Based on these SNPs, 6 main haplotypes (frequencies > 2%) were shown in detail in *indica* and *japonica* cultivars, with Hap 1 mainly present in *japonica* cultivars (87.08%) and only 1.21% in *indica* (Fig. 7B). The other haplotypes (Hap 2 to Hap 5) were major in *indica* cultivars with 35.78%, 30.93%, 23.60% and 6.31%, respectively (Fig. 7B). Seedling height was significantly different between *indica* and *japonica* cultivars, with Hap 1 and Hap 6 (the two main *japonica* haplotypes) showing 35.5 cm and 34.1 cm respectively, whereas Hap 2 to Hap 5 (the two main *indica*

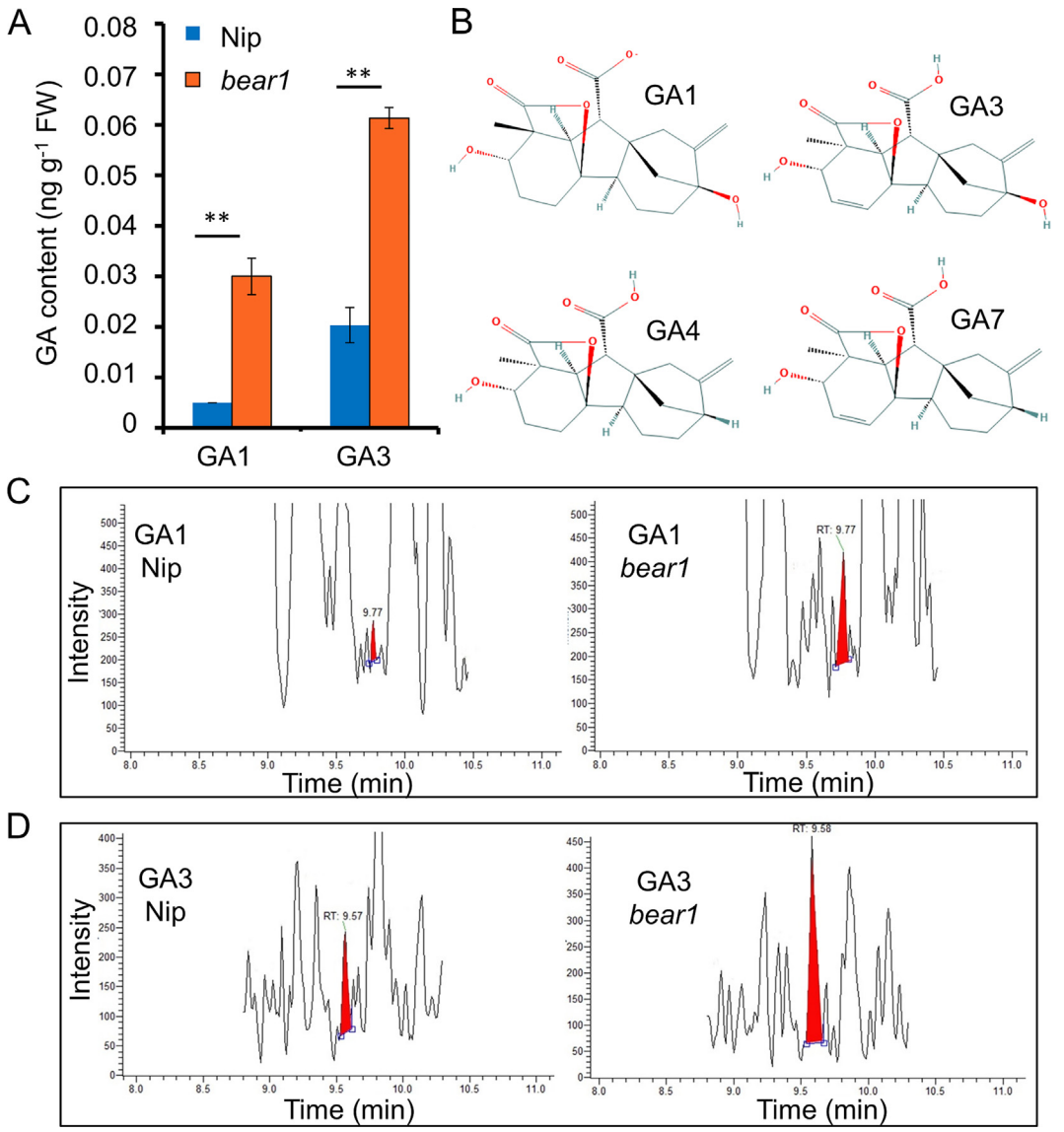

Fig. 4. Determination of endogenous active GAs content of Nip and *bear1* seedlings.
(A) Contents of endogenous GA_1 and GA_3 in Nip and *bear1* seedlings. Error bars represent SD ($n = 3$). *, $P < 0.05$; **, $P < 0.01$ (Student's *t*-test). (B) Molecular structure of active GAs. (C) Chromatograms of GA_1 in Nip and *bear1*. The red area represents the amount of GA_1. (D) Chromatograms of GA_3 in Nip and *bear1*. The red area represents the amount of GA_3.

haplotypes) showing seedling height from 38.1 cm to 41.2 cm (Fig. 7C). Plant height of these haplotypes had no obvious differences, which is consistent with the phenotype of *bear1* at mature stage. These results indicate that *BEAR1* has distinct haplotype differentiation between *indica* and *japonica* rice varieties, and is strongly associated with seedling height, implying a pivotal role of *BEAR1* in controlling height between *indica* and *japonica* cultivars.

4. Discussion

In this study, we collected four lines of evidence to support the notion that BEAR1 controls seedling height by functioning in GA biosynthesis pathway and inhibiting the expression of *OsKS4*. Firstly, we observed that the *BEAR1*-RNAi line and *bear1* CRISPR mutant displayed higher seedling phenotype compared to Nip. Secondly, qPCR results revealed that the expression of *OsKS4* and *OsCPS2* related to GA biosynthesis was significantly increased in the *bear1* mutant. Thirdly, the LC-MS/MS assay confirmed that the content of endogenous active GA was notably increased in *bear1* mutant. Finally, our molecular and biochemical experiments revealed that BEAR1 represses the expression of *OsKS4* by directly binding to its promoter. These findings enable us to conclude that BEAR1 binds to the promoter of *OsKS4* to inhibit its expression, which in turn regulates GA content and seedling height, thus resulting in the higher seedling of *bear1* mutant. These results deepen our understandings of the molecular mechanisms of bHLH transcription factor in regulating early seedling growth in rice.

4.1. Other possible function of BEAR1

Analysis of evolutionary data revealed that the genes most closely related to *BEAR1*, such as *OsGL3b*, *OSB1*, *OSB2*, *OsRb* and *OsRb2* (Fig. S2B), were all related to flavonoid and anthocyanin metabo-

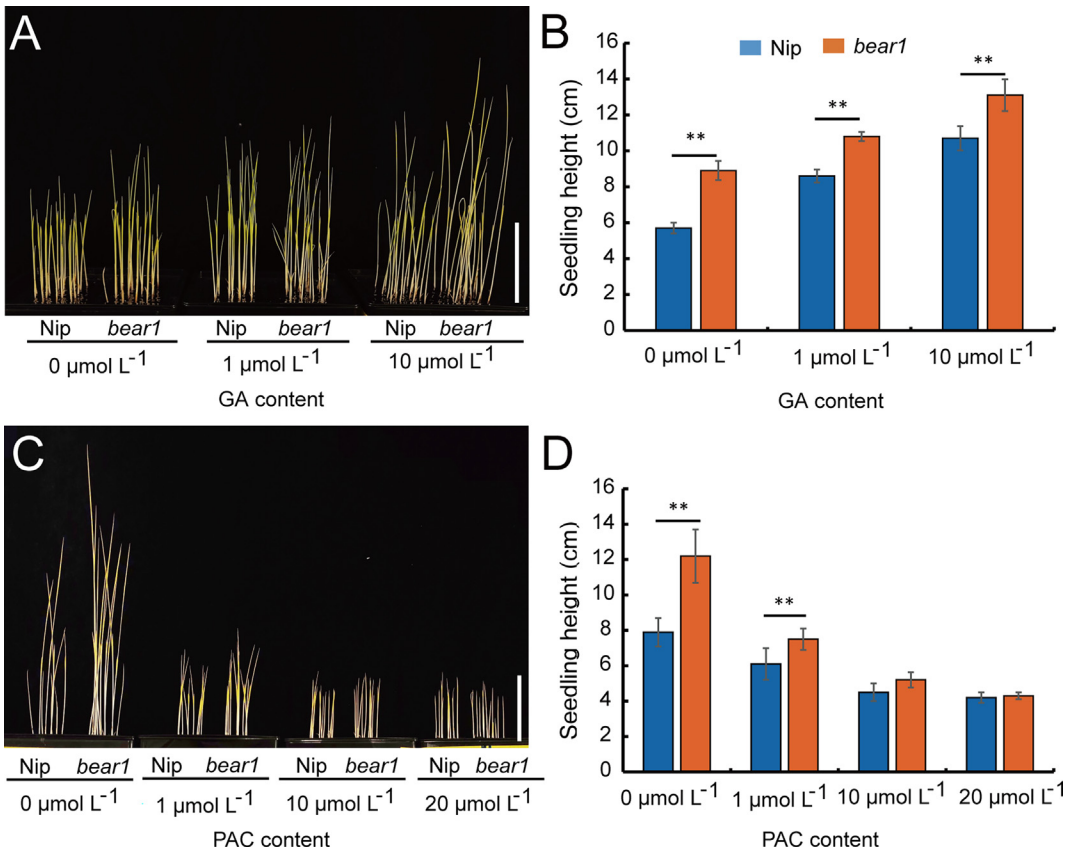

Fig. 5. Phenotypes of Nip and *bear1* under GA and PAC treatment.
(A, B) Seedling phenotypes (A) and height statistics (B) of Nip and *bear1* with different concentrations of GA treatment under the condition of 24 h darkness at 28 °C. *, $P < 0.05$; **, $P < 0.01$ (Student's *t*-test). (C, D) Seedling phenotypes (C) and height statistics (D) of Nip and *bear1* with range of concentrations of PAC treatment under the condition of 24 h darkness at 28 °C. *, $P < 0.05$; **, $P < 0.01$ (Student's *t*-test).

lism [51–53]. *GL3* and *EGL3* are homologous genes of *OsGL3b* in *Arabidopsis thaliana*, which not only participate in anthocyanin metabolism, but also in the regulation root development [54,55]. These clues suggest *BEAR1* may involve in a possible link between plant growth and anthocyanin metabolism.

4.2. Expression of BEAR1 at seedling stage

Expression profile analysis of qPCR and GUS staining revealed that *BEAR1* was preferentially expressed in the coleoptile and leaves of seedling. This was further corroborated by the significant phenotypes of CRISPR and RNAi mutants, indicating that *BEAR1* plays an important role in the regulation of rice growth and development and is strictly regulated. qPCR showed that the expression of BEAR1 significantly increased 8 days after germination (Fig. 3A), which was consistent with GUS staining results that GUS signal was also detected in seedlings at same stage (Fig. S6). Moreover, GUS signals were mostly distributed in the most active parts of seedlings, which was in agreement with the phenotype of *bear1*. We also checked the expression of *BEAR1* at mature stage. The GUS signal cannot be detected in roots, stem and leaves (Data not shown).

4.3. BEAR1 functions in GA metabolism

By analyzing the expression of genes related to GA biosynthesis and degradation, we found that 4 genes expression in GA degradation were up-regulated about 1.5–2 folds, and 3 genes were down-regulated to about 1/2. These results indicated that genes of GA degradation pathway had little changes in general, which suggested that GA2 degradation pathway may not be the main regulation pathway of *BEAR1*. For the gene expression in GA biosynthesis, four genes were significantly up-regulated (up to 3.5 folds), especially *CPS2* and *KS4* (Fig. 3), so we mainly studied the GA synthesis pathway regulated by *BEAR1*. Our further molecular and biochemical experiments also confirmed that BEAR1 regulates GA biosynthesis and inhibits the expression of *OsKS4* by binding to the P8 fragment of its promoter (Fig. 6). The *cis*-element analysis revealed that the P8 fragment in *OsKS4* promoter contained four conserved motifs, including W-box (GGTCAA), DRE core motif (GCCGACC), ABRE4 motif (CACGTA) and G-box (CACGTT) (Fig. S9). The G-box element was reported as the core DNA binding motif of the bHLH TF mainly binding site [56], which suggested that BEAR1 may bind to the promoter of *OsKS4* by directly binding the G-box motif.

4.4. The application of BEAR1

There are many mechanisms by which plants regulate seedling growth [57–59]. In recent reports, *gy1* mutant is similar to *bear1* mutant in many aspects, and its etiolated seedlings also show a longer and faster phenotype. GY1 plays a role in the early stage of JA synthesis and inhibits the elongation of the mesocotyl and coleoptile of seedlings by positively regulating JA synthesis and JA content, and acts as a growth suppressor just like BEAR1. The spatiotemporal expression conditions of *GY1* are also very strict, and the mutant *gy1* is only observed in the early stage of etiolated

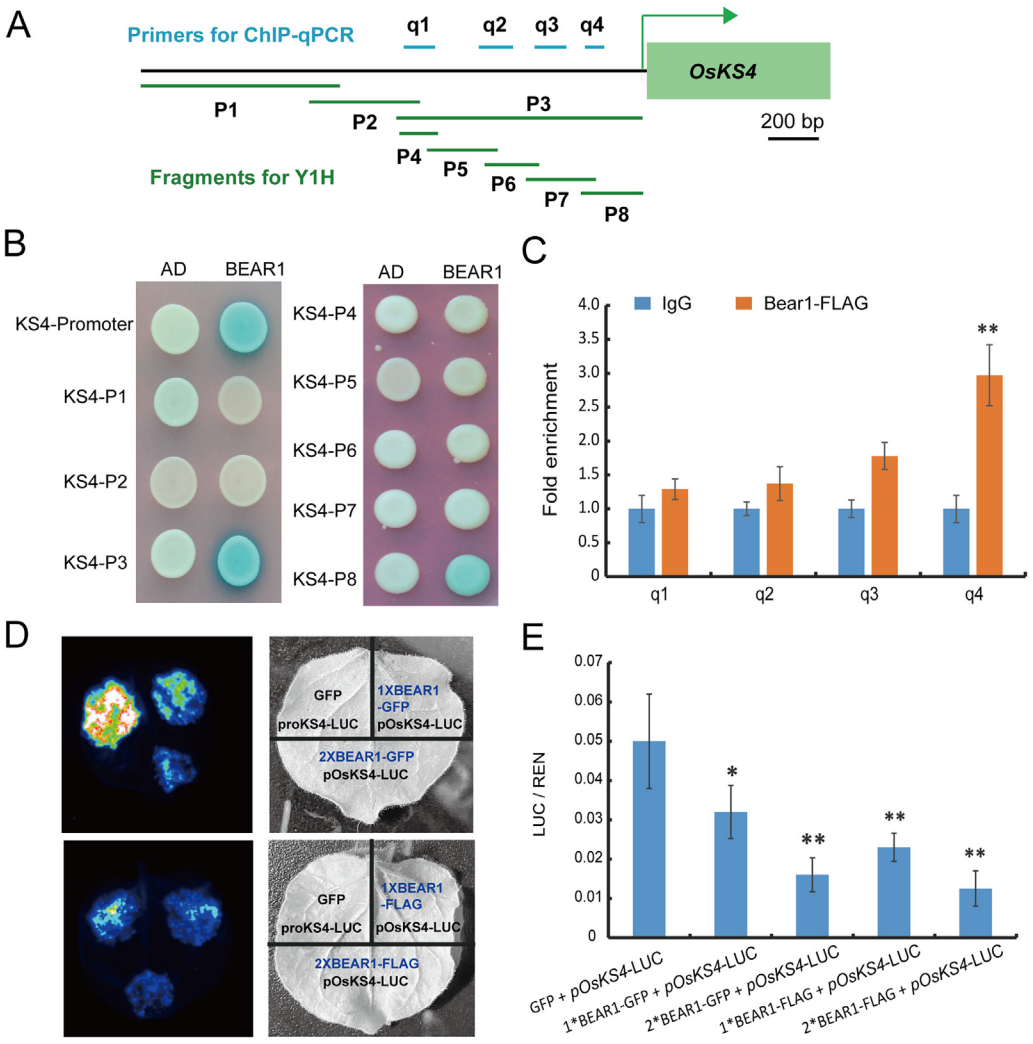

Fig. 6. BEAR1 represses the expression of *OsKS4* by directly binding to its promoter.
(A) Schematic depictions of the fragments in the promoter of *OsKS4*. (B) Y1H assay showed that BEAR1 can directly bind to the promoter of *OsKS4*. (C) ChIP-qPCR assay showed that BEAR1 had significant enrichment in the q4 region of *OsKS4* promoter. (D) Transient expression assay showed BEAR1 repressed the expression of *OsKS4* in *N. benthamiana* leaves (n = 3). (E) Dual-luciferase assay showed the relative LUC expression (n = 4). LUC/REN ration represents the relative activity of the promoters.

seedlings [60]. By contrast, phenotype of *bear1* is more obvious and is present in both photoperiod and dark environments (Figs. 1, 2).

BEAR1 has a promising application prospect, as demonstrated by the CRISPR mutant, which accelerates growth and development. This acceleration of growth at seedling stage can indirectly improve grain yield, making it useful for the cultivation and optimization of rice varieties.

CRediT authorship contribution statement

Yantong Teng: Data curation, Writing - original draft. **Maohong Cai:** Data curation, Formal analysis, Writing - review & editing, Funding acquisition. **Qinyu Xie:** Validation, Data curation. **Qinglong Liu:** Formal analysis. **Haiwen Zhang:** Writing - review & editing. **Tao Chen:** Project administration, Writing - review & editing, Funding acquisition.

Declaration of competing interest

The authors declare that they have no known competing financial interests or personal relationships that could have appeared to influence the work reported in this paper.

Acknowledgments

We thank Prof. Liming Xiong for manuscript editing. We thank Dr. Yangwen Qian and Dr. Pantong Zhang (Biogle Genome Editing Center) for the help in genome editing. We thank Wuhan Greensword Creation Technology Co., Ltd. for GAs measurement. This work was supported by the National Natural Science Foundation of China (32071932), Scientific Research Foundation for Scholars of HZNU (2019QDL015), and the Natural Science Foundation of Zhejiang province (LQ22C130001).

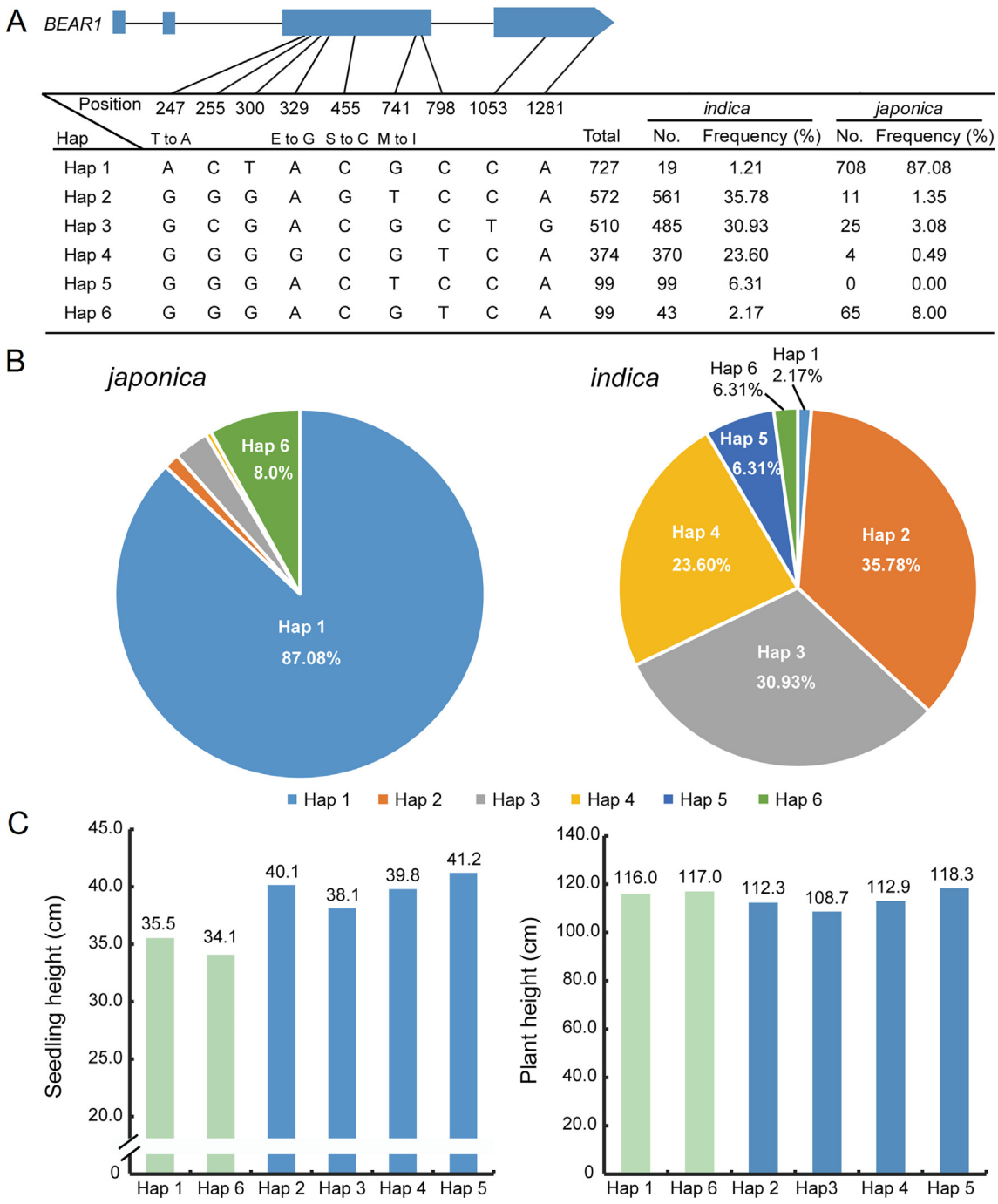

Hap	T to A			E to G	S to C	M to I				Total	*indica* No.	*indica* Frequency (%)	*japonica* No.	*japonica* Frequency (%)
Hap 1	A	C	T	A	C	G	C	C	A	727	19	1.21	708	87.08
Hap 2	G	G	G	A	G	T	C	C	A	572	561	35.78	11	1.35
Hap 3	G	C	G	A	C	G	C	T	G	510	485	30.93	25	3.08
Hap 4	G	G	G	G	C	G	T	C	A	374	370	23.60	4	0.49
Hap 5	G	G	G	A	C	T	C	C	A	99	99	6.31	0	0.00
Hap 6	G	G	G	A	C	G	T	C	A	99	43	2.17	65	8.00

Fig. 7. Haplotypes analysis of *BEAR1* associate with rice seedling height.
(A) The polymorphic nucleotides of *BEAR1* encoding region in *japonica* and *indica* cultivars. (B) Distribution of proportion of 6 haplotypes in *japonica* (left) and *indica* cultivars (right). (C) Seedling height and plant height statistics of 6 haplotypes.

Appendix A. Supplementary data

Supplementary data for this article can be found online at https://doi.org/10.1016/j.cj.2023.02.007.

References

[1] J. Itoh, K. Nonomura, K. Ikeda, S. Yamaki, Y. Inukai, H. Yamagishi, H. Kitano, Y. Nagato, Rice plant development: from zygote to spikelet, Plant Cell Physiol. 46 (2005) 23–47.

[2] S. Huang, L. Hu, S. Zhang, M. Zhang, W. Jiang, T. Wu, X. Du, Rice OsWRKY50 mediates ABA-dependent seed germination and seedling growth, and ABA-independent salt stress tolerance, Int. J. Mol. Sci. 22 (2021) 8625.

[3] S. Wang, W. Liu, Y. He, T.V. Adegoke, J. Ying, X. Tong, Z. Li, L. Tang, H. Wang, J. Zhang, Z.H. Tian, Y.F. Wang, bZIP72 promotes submerged rice seed germination and coleoptile elongation by activating ADH1, Plant Physiol. Biochem. 169 (2021) 112–118.

[4] J. Wang, H. Qin, S. Zhou, P. Wei, H. Zhang, Y. Zhou, Y. Miao, R. Huang, The ubiquitin-binding protein OsDSK2a mediates seedling growth and salt responses by regulating gibberellin metabolism in rice, Plant Cell 32 (2020) 414–428.

[5] W. Zhang, X. Zhou, C.K. Wen, Modulation of ethylene responses by *OsRTH1* overexpression reveals the biological significance of ethylene in rice seedling growth and development, J. Exp. Bot 63 (2012) 4151–4164.
[6] C.A. Lu, C.C. Lin, K.W. Lee, J.L. Chen, L.F. Huang, S.L. Ho, H.J. Liu, Y.I. Hsing, S.M. Yu, The SnRK1A protein kinase plays a key role in sugar signaling during germination and seedling growth of rice, Plant Cell 19 (2007) 2484–2499.
[7] Q. Lin, Z. Zhang, F. Wu, M. Feng, Y. Sun, W. Chen, Z. Cheng, X. Zhang, Y. Ren, C. Lei, S. Zhu, J. Wang, Z. Zhao, X. Guo, H. Wang, J. Wan, The APC/C(TE) E3 ubiquitin ligase complex mediates the antagonistic regulation of root growth and tillering by ABA and GA, Plant Cell 32 (2020) 1973–1987.
[8] M. de Lucas, J.M. Davière, M. Rodríguez-Falcón, M. Pontin, J.M. Iglesias-Pedraz, S. Lorrain, C. Fankhauser, M.A. Blázquez, E. Titarenko, S. Prat, A molecular framework for light and gibberellin control of cell elongation, Nature 451 (2008) 480–484.
[9] M. Kaneko, Y. Inukai, M. Ueguchi-Tanaka, H. Itoh, T. Izawa, Y. Kobayashi, T. Hattori, A. Miyao, H. Hirochika, M. Ashikari, M. Matsuoka, Loss-of-function mutations of the rice *GAMYB* gene impair alpha-amylase expression in aleurone and flower development, Plant Cell 16 (2004) 33–44.
[10] K. Aya, M. Ueguchi-Tanaka, M. Kondo, K. Hamada, K. Yano, M. Nishimura, M. Matsuoka, Gibberellin modulates anther development in rice via the transcriptional regulation of GAMYB, Plant Cell 21 (2009) 1453–1472.
[11] C.T. Kwon, N.C. Paek, Gibberellic acid: A key phytohormone for spikelet fertility in rice grain production, Int. J. Mol. Sci. 17 (2016) 794.
[12] D. Morrone, J. Chambers, L. Lowry, G. Kim, A. Anterola, K. Bender, R.J. Peters, Gibberellin biosynthesis in bacteria: separate ent-copalyl diphosphate and ent-kaurene synthases in *Bradyrhizobium japonicum*, FEBS Lett. 583 (2009) 475–480.
[13] M. Mizutani, D. Ohta, Diversification of P450 genes during land plant evolution, Annu. Rev. Plant Biol. 61 (2010) 291–315.
[14] D. Morrone, X. Chen, R.M. Coates, R.J. Peters, Characterization of the kaurene oxidase CYP701A3, a multifunctional cytochrome P450 from gibberellin biosynthesis, Biochem. J. 431 (2010) 337–344.
[15] C.A. Helliwell, P.M. Chandler, A. Poole, E.S. Dennis, W.J. Peacock, The CYP88A cytochrome P450, ent-kaurenoic acid oxidase, catalyzes three steps of the gibberellin biosynthesis pathway, Proc. Natl. Acad. Sci. U. S. A. 98 (2001) 2065–2070.
[16] T. Lange, P. Hedden, J.E. Graebe, Expression cloning of a gibberellin 20-oxidase, a multifunctional enzyme involved in gibberellin biosynthesis, Proc. Natl. Acad. Sci. U. S. A. 91 (1994) 8552–8556.
[17] S. Yamaguchi, Gibberellin metabolism and its regulation, Annu. Rev. Plant Biol. 59 (2008) 225–251.
[18] S.G. Thomas, A.L. Phillips, P. Hedden, Molecular cloning and functional expression of gibberellin 2- oxidases, multifunctional enzymes involved in gibberellin deactivation, Proc. Natl. Acad. Sci. U. S. A. 96 (1999) 4698–4703.
[19] J. Curaba, T. Moritz, R. Blervaque, F. Parcy, V. Raz, M. Herzog, G. Vachon, *AtGA3ox2*, a key gene responsible for bioactive gibberellin biosynthesis, is regulated during embryogenesis by LEAFY COTYLEDON2 and FUSCA3 in *Arabidopsis*, Plant Physiol. 136 (2004) 3660–3669.
[20] H. Wang, L.V. Caruso, A.B. Downie, S.E. Perry, The embryo MADS domain protein AGAMOUS-Like 15 directly regulates expression of a gene encoding an enzyme involved in gibberellin metabolism, Plant Cell 16 (2004) 1206–1219.
[21] T. Sakamoto, N. Kamiya, M. Ueguchi-Tanaka, S. Iwahori, M. Matsuoka, KNOX homeodomain protein directly suppresses the expression of a gibberellin biosynthetic gene in the tobacco shoot apical meristem, Genes Dev. 15 (2001) 581–590.
[22] E. Oh, S. Yamaguchi, J. Hu, J. Yusuke, B. Jung, I. Paik, H.S. Lee, T.P. Sun, Y. Kamiya, G. Choi, PIL5, a phytochrome-interacting bHLH protein, regulates gibberellin responsiveness by binding directly to the GAI and RGA promoters in *Arabidopsis* seeds, Plant Cell 19 (2007) 1192–1208.
[23] E. Oh, S. Yamaguchi, Y. Kamiya, G. Bae, W.I. Chung, G. Choi, Light activates the degradation of PIL5 protein to promote seed germination through gibberellin in *Arabidopsis*, Plant J. 47 (2006) 124–139.
[24] B. DeRybel, B. Möller, S. Yoshida, I. Grabowicz, P. BarbierdeReuille, S. Boeren, R. Smith, J. Borst, D. Weijers, A bHLH complex controls embryonic vascular tissue establishment and indeterminate growth in *Arabidopsis*, Dev. Cell 24 (2013) 426–437.
[25] C.A. MacAlister, K. Ohashi-Ito, D.C. Bergmann, Transcription factor control of asymmetric cell divisions that establish the stomatal lineage, Nature 445 (2007) 537–540.
[26] L.J. Pillitteri, D.B. Sloan, N.L. Bogenschutz, K.U. Torii, Termination of asymmetric cell division and differentiation of stomata, Nature 445 (2007) 501–505.
[27] V.C. Galvao, A.S. Fiorucci, M. Trevisan, J.M. Franco-Zorilla, A. Goyal, E. Schmid-Siegert, R. Solano, C. Fankhauser, PIF transcription factors link a neighbor threat cue to accelerated reproduction in *Arabidopsis*, Nat. Commun. 10 (2019) 4005.
[28] B. Feng, D. Lu, X. Ma, Y. Peng, Y. Sun, G. Ning, H. Ma, Regulation of the *Arabidopsis* anther transcriptome by DYT1 for pollen development, Plant J. 72 (2012) 612–624.
[29] S.V. Kumar, D. Lucyshyn, K.E. Jaeger, E. Alós, E. Alvey, N.P. Harberd, P.A. Wigge, Transcription factor PIF4 controls the thermosensory activation of flowering, Nature 484 (2012) 242–245.
[30] C. Ji, H. Li, L. Chen, M. Xie, F. Wang, Y. Chen, Y.G. Liu, A novel rice bHLH transcription factor, DTD, acts coordinately with TDR in controlling tapetum function and pollen development, Mol. Plant 6 (2013) 1715–1718.
[31] C. Bernhardt, M.M. Lee, A. Gonzalez, F. Zhang, A. Lloyd, J. Schiefelbein, The bHLH genes *GLABRA3 (GL3)* and *ENHANCER OF GLABRA3 (EGL3)* specify epidermal cell fate in the *Arabidopsis* root, Development 130 (2003) 6431–6439.
[32] P. Leivar, E. Monte, PIFs: systems integrators in plant development, Plant Cell 26 (2014) 56–78.
[33] I. Paik, F. Chen, V. Ngoc Pham, L. Zhu, J.I. Kim, E. Huq, A phyB-PIF1-SPA1 kinase regulatory complex promotes photomorphogenesis in *Arabidopsis*, Nat. Commun. 10 (2019) 4216.
[34] A. Sharma, B. Sharma, S. Hayes, K. Kerner, U. Hoecker, G.I. Jenkins, K.A. Franklin, UVR8 disrupts stabilisation of PIF5 by COP1 to inhibit plant stem elongation in sunlight, Nat. Commun. 10 (2019) 4417.
[35] J. Oh, E. Park, K. Song, G. Bae, G. Choi, PHYTOCHROME INTERACTING FACTOR8 inhibits phytochrome a-mediated far-red light responses in *Arabidopsis*, Plant Cell 32 (2020) 186–205.
[36] Y. Hyun, I. Lee, KIDARI, encoding a non-DNA Binding bHLH protein, represses light signal transduction in *Arabidopsis thaliana*, Plant Mol. Biol. 61 (2006) 283–296.
[37] J.W. Chandler, M. Cole, A. Flier, W. Werr, BIM1, a bHLH protein involved in brassinosteroid signalling, controls *Arabidopsis* embryonic patterning via interaction with DORNRÖSCHEN and DORNRÖSCHEN-LIKE, Plant Mol. Biol. 69 (2009) 57–68.
[38] Y.E. Xie, H. Tan, Z. Ma, J. Huang, DELLA proteins promote anthocyanin biosynthesis via sequestering MYBL2 and JAZ suppressors of the MYB/bHLH/WD40 complex in *Arabidopsis thaliana*, Mol. Plant 9 (2016) 711–721.
[39] Z. Feng, B. Zhang, W. Ding, X. Liu, D.L. Yang, P. Wei, F. Cao, S. Zhu, F. Zhang, Y. Mao, J.K. Zhu, Efficient genome editing in plants using a CRISPR/Cas system, Cell Res. 23 (2013) 1229–1232.
[40] Y. Hiei, T. Komari, Agrobacterium-mediated transformation of rice using immature embryos or calli induced from mature seed, Nat. Protoc. 3 (2008) 824–834.
[41] A. Waterhouse, M. Bertoni, S. Bienert, G. Studer, G. Tauriello, R. Gumienny, F.T. Heer, T.A.P. de Beer, C. Rempfer, L. Bordoli, R. Lepore, T. Schwede, SWISS-MODEL: homology modelling of protein structures and complexes, Nucleic Acids Res. 46 (2018) W296–W303.
[42] S. El-Gebali, J. Mistry, A. Bateman, S.R. Eddy, A. Luciani, S.C. Potter, M. Qureshi, L.J. Richardson, G.A. Salazar, A. Smart, E.L.L. Sonnhammer, L. Hirsh, L. Paladin, D. Piovesan, S.C.E. Tosatto, R.D. Finn, The Pfam protein families database in 2019, Nucleic Acids Res. 47 (2019) D427–D432.
[43] N. Hulo, A. Bairoch, V. Bulliard, L. Cerutti, E. De Castro, P.S. Langendijk-Genevaux, M. Pagni, C.J. Sigrist, The PROSITE database, Nucleic Acids Res. 34 (2006) D227–D230.
[44] S. Kumar, G. Stecher, M. Li, C. Knyaz, K. Tamura, MEGA X: molecular evolutionary genetics analysis across computing platforms, Mol. Biol. Evol. 35 (2018) 1547–1549.
[45] P.B. Brewer, M.G. Heisler, J. Hejátko, J. Friml, E. Benková, In situ hybridization for mRNA detection in *Arabidopsis* tissue sections, Nat. Protoc. 1 (2006) 1462–1467.
[46] T. Nolan, R.E. Hands, S.A. Bustin, Quantification of mRNA using real-time RT-PCR, Nat. Protoc. 1 (2006) 1559–1582.
[47] B.D. Cai, J. Yin, Y.H. Hao, Y.N. Li, B.F. Yuan, Y.Q. Feng, Profiling of phytohormones in rice under elevated cadmium concentration levels by magnetic solid-phase extraction coupled with liquid chromatography tandem mass spectrometry, J. Chromatogr. A. 1406 (2015) 78–86.
[48] R. Lin, L. Ding, C. Casola, D.R. Ripoll, Cédric Feschotte, H. Wang, Transposase-derived transcription factors regulate light signaling in *Arabidopsis*, Science 318 (2007) 1302–1305.
[49] Y. Xie, Y. Liu, H. Wang, X. Ma, B. Wang, G. Wu, H. Wang, Phytochrome-interacting factors directly suppress *MIR156* expression to enhance shade-avoidance syndrome in *Arabidopsis*, Nat. Commun. 8 (2017) 348.
[50] E. Duan, Y. Wang, X. Li, Q. Lin, T. Zhang, Y. Wang, C. Zhou, H. Zhang, L. Jiang, J. Wang, C. Lei, X. Zhang, X. Guo, H. Wang, J. Wan, *OsSHI1* regulates plant architecture through modulating the transcriptional activity of *IPA1* in rice, Plant Cell 31 (2019) 1026–1042.
[51] C.H. Shih, H. Chu, L.K. Tang, W. Sakamoto, M. Maekawa, I.K. Chu, M. Wang, C. Lo, Functional characterization of key structural genes in rice flavonoid biosynthesis, Planta 228 (2008) 1043–1054.
[52] J. Zheng, H. Wu, H. Zhu, C. Huang, C. Liu, Y. Chang, Z. Kong, Z. Zhou, G. Wang, Y. Lin, H. Chen, Determining factors, regulation system, and domestication of anthocyanin biosynthesis in rice leaves, New Phytol. 223 (2019) 705–721.
[53] K. Zheng, X. Wang, Y. Wang, S. Wang, Conserved and non-conserved functions of the rice homologs of the *Arabidopsis* trichome initiation-regulating MBW complex proteins, BMC Plant Biol. 21 (2021) 234.
[54] C. Bernhardt, M. Zhao, A. Gonzalez, A. Lloyd, J. Schiefelbein, The bHLH genes *GL3* and *EGL3* participate in an intercellular regulatory circuit that controls cell patterning in the *Arabidopsis* root epidermis, Development 132 (2005) 291–298.
[55] X.C. Wang, J. Wu, M.L. Guan, C.H. Zhao, P. Geng, Q. Zhao, *Arabidopsis MYB4* plays dual roles in flavonoid biosynthesis, Plant J. 101 (2020) 637–652.
[56] X. Li, X. Duan, H. Jiang, Y. Sun, Y. Tang, Z. Yuan, J. Guo, W. Liang, L. Chen, J. Yin, H. Ma, J. Wang, D. Zhang, Genome-wide analysis of basic/helix-loop-helix transcription factor family in rice and *Arabidopsis*, Plant Physiol. 141 (2006) 1167–1184.
[57] J. Ponnu, Molecular mechanisms suppressing COP1/SPA E3 ubiquitin ligase activity in blue light, Physiol. Plant. 169 (2020) 418–429.

[58] T.M. Nolan, N. Vukasinovic, D. Liu, E. Russinova, Y. Yin, Brassinosteroids: multidimensional regulators of plant growth, development, and stress responses, Plant Cell 32 (2020) 295–318.
[59] M. Salehin, R. Bagchi, M. Estelle, SCFTIR1/AFB-based auxin perception: mechanism and role in plant growth and development, Plant Cell 27 (2015) 9–19.
[60] Q. Xiong, B. Ma, X. Lu, Y.H. Huang, S.J. He, C. Yang, C.C. Yin, H.E. Zhao, Y. Zhou, W.K. Zhang, W.S. Wang, Z.K. Li, S.Y. Chen, J.S. Zhang, Ethylene-inhibited jasmonic acid biosynthesis promotes mesocotyl/coleoptile elongation of etiolated rice seedlings, Plant Cell 29 (2017) 1053–1072.